UC-413
LBL-27983

Lawrence Berkeley Laboratory
UNIVERSITY OF CALIFORNIA

Invited paper presented at the American Chemical Society Meeting, Symposium on Exotic Nuclear Spectroscopy, Miami Beach, FL, September 11–15, 1989

Rotational Population Patterns and Searches for the Nuclear SQUID

L.F. Canto, R.J. Donangelo, A.R. Farhan, M.W. Guidry, J.O. Rasmussen, P. Ring, and M.A. Stoyer

November 1989

NUCLEAR SCIENCE DIVISION

For Reference

Not to be taken from this room

LBL-27983
Copy 1
Bldg. 50 Library.

Prepared for the U.S. Department of Energy under Contract Number DE-AC03-76SF00098.

DISCLAIMER

This document was prepared as an account of work sponsored by the United States Government. While this document is believed to contain correct information, neither the United States Government nor any agency thereof, nor the Regents of the University of California, nor any of their employees, makes any warranty, express or implied, or assumes any legal responsibility for the accuracy, completeness, or usefulness of any information, apparatus, product, or process disclosed, or represents that its use would not infringe privately owned rights. Reference herein to any specific commercial product, process, or service by its trade name, trademark, manufacturer, or otherwise, does not necessarily constitute or imply its endorsement, recommendation, or favoring by the United States Government or any agency thereof, or the Regents of the University of California. The views and opinions of authors expressed herein do not necessarily state or reflect those of the United States Government or any agency thereof or the Regents of the University of California.

Rotational Population Patterns and Searches for the Nuclear SQUID

L.F.Canto**, R.J.Donangelo**, A.R.Farhan%, M.W.Guidry#,
J.O.Rasmussen*, P.Ring+, and M.A.Stoyer*

ABSTRACT

This paper presents new theoretical results for rotational population patterns in the nuclear SQUID effect. (The term nuclear SQUID is in analogy to the solid-state Superconducting Quantum Interference Devices.) The SQUID effect is an interesting new twist to an old quest to understand Coriolis anti-pairing (CAP) effects in nuclear rotational bands. Two-neutron transfer reaction cross sections among high-spin states have long been touted as more specific CAP probes than other nuclear properties. Heavy projectiles like Sn or Pb generally are recommended to pump the deformed nucleus to as high spin as possible for transfer. The interference and sign reversal of 2n transfer amplitudes at high spin, as predicted in the early SQUID work imposes the difficult requirement of Coulomb pumping to near back-bending spins at closest approach. For Pb on rare earths we find a dramatic departure from sudden-approximation, so that the population depression occurs as low as final spin 10h.

1.1 INTRODUCTION

The acronym SQUID stands for Superconducting Quantum Interference Device, a solid-state device exploiting quantum aspects of superconductivity. Ring and Nikam[1] suggested that a nuclear analogy might exist in the 2-neutron transfer reaction between heavy ions, where one of the nuclei is deformed and excited to a high rotational state by Coulomb excitation. In the solid state case Josephson currents are affected by a superimposed magnetic field. In the nuclear case the pair supercurrent between the nuclei is affected by the rotational field. The idea was developed further by the above authors and others in subsequent papers[2,3].

It has long been generally believed that the increase of moment of inertia at higher spin in most deformed nuclei is caused mainly by a decrease in the pairing correlation at higher rotational velocities, the so-called Coriolis antipairing (CAP) effect. It was suggested[4] that this CAP effect could be tested by 2-neutron transfer reactions between heavy nuclei, the Coulomb excitation on the inward path pumping the deformed partner into higher rotational states from which the 2-n transfer occurs. Pair transfer is strongly enhanced by the pairing correlation, the enhancement factor being essentially the square of the number of Nilsson orbitals involved in pair configuration mixing. The ground-to-ground enhancement factor is given by the following:

$$F = \sum_{i>0} {}_{A}u_i \; {}_{A+2}v_i \approx \sum {}_{A}u_i \, {}_{A}v_i = \frac{\Delta}{G} \qquad (1)$$

where v and u are the BCS fullness and emptiness amplitudes, respectively. What was envisioned in this earlier time was that 2n

transfer would steadily and monotonically weaken with increasing spin.

The new and interesting aspect of the SQUID effect prediction is that the pair transfer matrix element decreases through zero and changes sign. To see this effect strongly it is thought that the Coulomb excitation on the inward path must excite to near the backbending spin (diabolic point). The cancellation in 2n transfer matrix elements has been related to the Berry phase[5,6] in passing around the diabolic point in spin and particle-number space. Because of the very large Coulomb excitation required, attention has focussed on the heaviest spherical projectiles in the Pb region and targets in the deformed rare earth region. Semiclassical trajectory theoretical estimates of Landowne et al.[7] make it appear that in the most favorable case the SQUID effect will be a small decrease in the population of the highest rotational states--thus difficult to achieve and to prove. However, as our new method described below shows, the sudden approximation used in Ref. 7 is not applicable for systems with such a high-Z projectile as Pb, and the theoretical rotational population decrease from the SQUID effect should occur at half the spin given by the sudden approximation.

We have undertaken two new approaches to the transfer theory. First, we have considered the dependence of transfer on the zones of the most lightly bound $i_{13/2}$ Nilsson orbitals on the surface of the deformed nucleus. The transfer strength over the surface is

taken as a product of factors, the WKB tunneling factor, the absorption factor, and the square of Nilsson wave functions of the most lightly bound orbitals. Second, we have moved a step to more quantal theory by adapting the Coulomb excitation codes originating with DeBoer and Winther,[8] where the collision partners move on a Rutherford hyperbolic orbit during integration of the time-dependent Schrodinger equation for the amplitudes of the various rotational states. In our new approach this integration is paused at closest approach, and the rotational amplitude vector is matrix-multiplied by a transfer matrix, taking into account transfer changing angular momentum as well as S-wave transfer. The characteristic 2n-tunneling length is sufficiently small that this approximation that transfer occurs at the classical turning point should be justified. After matrix multiplication accounting for transfer, tunneling distance, and nuclear optical potential absorption and phase shifts the DeBoer-Winther integration continues on the outward path to give the final rotational signature. (We learned recently that Pollarolo, Dasso, and deBoer are also studying the pair transfer process by similar modifications of the old Coulomb excitation codes. They confine their calculations to energies below the Coulomb barrier, where they feel it is safe not to include effects of the nuclear optical potential. They also have not included the effect of the oscillatory Nilsson wave functions over the nuclear surface.[9])

1.2 E2 COULOMB EXCITATION OF GROUND AND S-BAND

We may confidently apply semi-classical trajectory methods to estimate the amount of rotational angular momentum carried in by head-on heavy ion collisions. The higher the beam energy the higher the angular momentum up to the limit imposed by the Coulomb barrier. Above barrier the collision system predominantly goes into compound nucleus and other complex reaction channels, robbing flux from the simple transfer and rotational inelastic channels. For transfer reactions we are concerned with rotational angular momentum pumped in during the inward path, which is half the final Coulomb excited spin in the sudden limit. Guidry et al.[10] made such estimates for two deformed nuclei ^{156}Gd and ^{238}U with four different projectiles ranging from ^{16}O to ^{208}Pb, and these probability distributions are shown in Fig. 1. As backbending can occur in the rare earth region as low as spin 12h, we see that with ^{208}Pb as a projectile it should be possible to pump the rotational energy up to this region on the inward path. The nuclear rotor in the semiclassical calculations of ref. 7 did not deal with Coulomb excitation behavior in the backbending region.

The backbending region in the yrast band may best be thought of as a virtual band crossing, where an upper S-band with substantial aligned angular momentum crosses below the regular ground band. In the rare earth region the first backbend is with an S-band having two $i_{13/2}$ neutrons with angular momentum partially aligned along the rotational angular momentum axis and perpendicular to the cylindrical symmetry axis of the prolate spheroidal nucleus. In only a few cases has it been possible

experimentally to study electric quadrupole transition rates, i.e., B(E2), values within and between S- and ground bands.[11] The B(E2) values evidently are strongest among the yrast levels, with B(E2) values to the next band substantially lower. It can be shown that this behavior is to be expected unless backbending is so sharp that there is a sharp change in the wave function mixture of yrast levels from one level to the next. Thus, in our work to date we have not explicitly taken into account Coulomb excitation into the band above yrast, but it is straightforward with the deBoer-Winther amplitude method to incorporate detailed energies and B(E2) values in the backbending region of interest in our new calculations of diabolic pair transfer and the Squid effect.

1.3 DIABOLICAL POINTS AND THE NUCLEAR SQUID

In this paper there is not time to review in great detail the literature of the proposed nuclear squid effect, but we wish to give an overview of the highlights. Our Fig. 2 is taken from Fig. 3.2 of Ring[12]. The right-hand portion of the figure shows schematically two paths of (inward Coulex)/(2n transfer)/(outward Coulex) for nuclei of mass numbers A and A+2, respectively. One path (solid arrow) passes beneath the backbending, or diabolic, point and the other (dashed arrow) passes above. These paths are supposed to contribute to 2n transfer with opposite signs, hence cause a destructive interference in the 2n-transfer matrix element. The left-hand part of the figure is a diagram showing schematically where the diabolic points for the $i_{13/2}$ shell appear. The abscissa

is particle-number (or chemical potential λ), and the ordinate is rotational angular velocity (ω). Of course, these are really not continuous variables in real nuclei, but they are continuous in some of the general theoretical methods. That is, cranking velocity and angular momentum are continuous variables in deformed-nuclear-potential and cranking models, where spherical symmetry is broken. Likewise, particle number is not conserved in pairing models like the BCS (Bardeen-Cooper-Schrieffer), where gauge symmetry is broken. The lower leftmost dot in our Fig. 2 represents the first band-crossing for spheroidal nuclei with chemical potential close to the $i_{13/2}$, Ω=3/2 Nilsson orbital. The Squid interference diagrammed at the right might then be expected for the A nucleus with chemical potential just below the 13/2;3/2 state and the A+2 nucleus just above. The upper four diabolic points are of purely mathematical interest, as angular momenta in this second 13/2 backbend region could not be realized experimentally in nuclei for transfer studies.

The earlier theoretical work on the Squid effect focussed on S-wave transfer in which there is no change in spin intrinsic to the transfer process at closest approach. However, we know from theory of alpha decay of deformed nuclei that a non-uniform emission or cluster transfer wave function over the nuclear surface necessarily implies angular-momentum changes. In particular here if we can specify the angular function over the surface that transforms incoming waves to outgoing transfer waves, we can

readily convert this to a square matrix transforming incoming deBoer-Winther amplitudes to outgoing transfer wave amplitudes. The angular transfer function is sandwiched between initial and final rotational functions and integrated over the Eulerian angles.

$$T_{\ell\ell'} = \int Y^*_{\ell' 0} \; F(\theta) \; Y_{\ell 0} \; \sin\theta \; d\theta \; d\varphi \qquad (2)$$

1.4 SURFACE ANGULAR FORM FACTOR OF PAIR TRANSFER

The concept of the angular form factor $F(\underline{x})$ ($\underline{x}=\cos\Theta$) was introduced in Ref. 3, although it was there incorporated into an angular projection integral for the classical limit S-matrix in the sudden approximation. In Eq. (4) of that work $F(\underline{x})$ was taken to be the product of three real factors, a 2n-tunneling factor $\underline{a}_{tunl}(\underline{x})$, an absorption factor $a_{abs}(x)$, and the squid spectroscopic factor $a_{spec}(I(x))$. The tunneling factor is just the WKB exponential for a 2-neutron cluster with experimental separation energy tunneling between surfaces at the classical distance of closest approach at angle Θ. Since in Ref. 3 and the present work we do not purport to compute absolute tunneling, only relative rotational populations, the pre-exponential factor is left at unity. The absorption factor in Ref. 3 is just a semiclassical trajectory time integral over the imaginary part of the optical potential. In the current work we make this factor complex by integrating over the complex optical potential, thus introducing phase shifts coming from the tail of

the real part of the nuclear potential. Figs. 3 and 4 are examples of tunneling and absorption factors at two bombarding energies for ^{208}Pb on ^{160}Dy. Only the absolute value of the absorption amplitude is plotted. Note that at the higher bombarding energy the absorption becomes very strong as one approaches the tip of the prolate nucleus, the right-hand side of the figure, since the abscissa is the cosine of theta. It is implicit in the form of the a_{abs} integral of Eq. (6) in Ref. 3 that the Q value of the reaction is taken to be zero. In fact, non-zero Q values could be incorporated, though we have not yet done so, by including in the time integral the factor exp(iQt/h), thus,

$$a_{abs} = \exp\left[-\frac{1}{i\hbar}\int_{-\infty}^{\infty}\left(V(t) + iW(t)\right) e^{\frac{iQt}{\hbar}}\, dt\right] \quad (3)$$

Likewise, the tunneling integral of Eq. (5) in Ref. 3 could easily be modified for non-zero Q values by inclusion of such a factor in the time integral for semiclassical tunneling, as done long ago by Breit and Ebel.[13]

$$a_{tunl} = C \exp\left[-\frac{2(2M_n)^{\frac{1}{2}}}{\hbar}(S_{2n})^{\frac{1}{2}}\int_0^{\infty}\frac{dx}{dt}\, e^{\frac{iQt}{\hbar}}\, dt\right], \quad (4)$$

where $x(t) = r(t) - R_p - R_t$, S_{2n} is the two-neutron binding energy, M_n is the neutron mass, C is an arbitrary constant, and Q is the energy release in the transfer reaction.

Next, we address a central matter of this paper, the Squid factor $\underline{a}_{spec}(\underline{I})$. S-wave matrix elements for pair transfer between

cranked HFB wave functions were found to cross through zero and go negative at about the spin where backbending or upbending occurs in the energy levels. The S-wave 2n-transfer matrix elements are as follows:

$$P = \langle A+2 \mid S^{+} \mid A \rangle ,$$

where the pair creation operator is

$$S^{+} = (a^{+} a^{+})_{I=0} ,$$

with a+ the neutron creation operators.

We show in Fig. 5 the results from Ref. 3 for deformed nucleus ^{160}Dy. The solid line gives the pair transfer matrix elements, and the dashed line is the pairing gap parameter, which only gradually decreases. As mentioned in the introduction, the oscillatory behavior of the transfer matrix elements shows up with realistic cranked HFB calculations comprising more than one oscillator shell, but it is the high-j intruder orbital $i_{13/2}$ that is mainly responsible, and cranked HFB solutions with just this orbital show qualitatively the same behavior.

It is possible to understand microscopically the origin of the effect in terms of just the three nearest $i_{13/2}$ Nilsson states nearest the Fermi energy in initial and final nuclei. At zero spin the pairing force makes the ground states a coherent mixture of the

various pair arrangements in the three orbitals, and the well-known superfluid pair transfer enhancement occurs. At increasing cranking velocity a second-order Coriolis term through the K=1+ intermediate states begins to oppose the pairing force mixture. The S-band in a weak-pairing limit at low spin is just the band derived from ground by promotion of one pair in the $i_{13/2}$ family from the Nilsson level just below the Fermi energy to the Nilsson level just above. (For strong pairing the S-band structure is a little more complicated, derivable in the number-conserving space by matrix diagonalization. It is expressible in HFB by a linear combination of quasiparticle operators mainly operating on the Nilsson orbitals nearest the Fermi energy.) With increasing spin the $i_{13/2}$ pairing coherence in ground is steadily reduced by the Coriolis interaction until the principal pairing-admixed term goes through zero and changes sign, usually before the virtual band crossing. (In sharp backbending cases the pairing mixing cancellation comes at about the same angular velocity as the band crossing.) The overall pair transfer matrix element is still positive when the admixed term first goes through zero. As the angular velocity of band crossing is approached, the negative admixed terms become comparable to the formerly dominant term, and the pair transfer for S-waves goes through zero, as shown in Fig. 5. Although the S-wave transfer goes through zero near band-crossing, that does not mean that the transfer amplitude is everywhere zero over the nuclear surface. The simple model discussed above suggests indeed a strongly oscillatory transfer amplitude over the nuclear surface near the diabolic point, since

there is a subtraction of the pair transfer from successive Nilsson $i_{13/2}$ states. At the deadline time of this paper we have not yet completed checking the surface angular form factors for transfer using cranked HFB $i_{13/2}$ wave functions, but it is clear that there are strong oscillations near the diabolic region. The results of theoretical rotational population patterns we present in the next section are preliminary in the sense that we approximate the angular transfer form factor by the product of the a_{spec} of Fig. 5 and Ref. 3 times the square of a spherical harmonic $|Y_{6\ 1}|^2$. The oscillatory form factor produces considerable angular-momentum change intrinsic to the transfer at closest approach.

1.5 NUMERICAL RESULTS--SQUID SIGNATURE IN ROTATIONAL POPULATION

When the form factors above are used with our modified deBoer-Winther transfer code, we find a remarkable effect of the Squid sign reversal at unexpectedly low spin for ^{210}Pb on ^{160}Dy at E_{lab}= 1200 MeV. Fig. 6 shows the rotational population pattern with and without the sign reversing a_{spec}. With the squid effect factor there is a considerable suppression in the population around spin 10h. We may gain an understanding of the reasons by examining the semiclassical trajectory quantum number functions, even though they are not now used in the population calculation. Fig. 7 shows for head-on collisions the spin at closest approach (solid line) and at infinite time (dashed line) as a function of initial orientation of the deformed nucleus. For small initial angles we see nearly the

behavior of the sudden approximation. That is, the final rotational angular momentum is nearly twice that at closest approach. However, a very different behavior is seen beyond 20° due to the finite rotation of the nucleus during the collision. Near 50° I_f crosses under $I_{c.a.}$, since the deformed nucleus can rotate past 90° during the collision and thus reverse the sign of the torque. The squid-effect removal of transfer amplitudes at closest approach near spins 10 to 12 translates to removal of rotational population at the same or slightly lower spin. The importance of treating the adiabatic dynamics of the collision instead of using the sudden approximation is quite clear. The special simplicity of the rotational pattern at 1200 MeV is evidently also a consequence of being enough above the barrier that the a_{abs} absorption factor effectively removes the small-angle root from contributing. When the bombarding energy is lowered to 1100 MeV, nuclear absorption is not so strong, as seen by comparing Figs.3 and 4, and both roots contribute, as evidenced by the oscillating population pattern of Fig. 8. These intensity oscillations are characteristic of the interference between the two roots of the quantum number function, as is well known in simple multiple Coulomb excitation.

We should remark here that the population suppression around spin 10h seems to require an oscillatory angular form factor near band crossing, though the final results do not depend much on whether m=0, 1, or 2 is taken for the spherical harmonic. If the spherical harmonic function is omitted, the population suppression is barely evident at all. The large size of the spherical

collision partner is expected to smear a sharply oscillating angular transfer strength and hence somewhat reduce the L transfer intrinsic to the transfer process, but we are still studying these modifications.

Space limitations of this paper preclude showing the corresponding population patterns and quantum number functions we calculated for Sn on Dy systems. Suffice it to say that the rotation barely exceeds the diabolic spin of ca. 12h for orientations in the 25-45° range. The population suppression occurs only in the final Coulomb excitation rainbow maximum around spin 16h.

In another paper of this symposium by one of us (M.W.Guidry) a puzzling new inhibition of high-spin 2n transfer was presented.14 This inhibition for Ni on Dy begins to cut in around spin 4 and reduces the population pattern to quite small by spin 10. We are trying to understand the origin of this inhibiting factor, which does not appear in the cranked HFB. If this FDSM inhibiting factor must be included, then the experimental proof of the nuclear SQUID effect will be harder, though perhaps still possible by careful comparison of transfer population patterns with a range of projectiles, such as, Ni, Sn, and Pb.

We hope soon to submit a short paper presenting the cranked HFB results with these new methods. Our preliminary calculations of HFB population patterns appear similar to those presented here.

1.6 Acknowledgements

The main support for this research came from the Director, Office of Energy Research, Division of Nuclear Physics of the Office of High Energy and Nuclear Physics of the U.S. Department of Energy under contract DE-AC03-76SF00098. We acknowledge also the essential travel support of a U.S.-Brazil cooperative research grant INT-8302853 of the U. S. National Science Foundation and the Brazilian Conselho Nacional de Pesquisas e Desenvolvimento Cientifico.

Figure Legends

Fig. 1. Calculations of the distribution of rotational angular momentum at closest approach for two spheroidal target nuclei and four spherical projectiles, from left to right ^{16}O, ^{58}Ni, ^{120}Sn, and ^{208}Pb. These calculations are made by classical trajectory methods in head-on collisions of energy causing the nuclei to barely touch. The figure is taken from Ref. 10.

Fig. 2. The left-hand portion of the figure is a schematic representation of the diabolic points of the $i_{13/2}$ Nilsson orbital family in the plane of particle number (chemical potential) and rotational angular momentum. The right hand rotational band scheme illustrates the principal interfering paths of Coulomb excitation

and 2n-transfer below and above the first diabolic point. This figure is taken from Ref. 2 (Phys. Lett.)

Fig. 3. Factors in the transfer matrix integrand over the spheroidal nuclear surface. The abscissa is cos Θ. The solid circles give the absorption factor arising from the tail of the imaginary component of the optical potential. The open circles are the tunneling amplitude factor. The squares represent the product of the two factors. These factors were calculated for ^{208}Pb on ^{160}Dy at a laboratory energy of 1100 MeV.

Fig. 4. Same as Fig. 3, except calculated for a beam energy of 1200 MeV, sufficiently near the top of the barrier that the absorption amplitude factor is as small as 0.2 (96% absorption) even at the equator, with very high absorption prevailing toward the poles.

Fig. 5. Calculated neutron pair transfer (L=0) matrix elements (solid line) as a function of spin. The traditional pair transfer sum of uv products (dashed line.) This calculation and figure is from Ref. 3.

Fig. 6. Calculated yrast rotational transfer population patterns for ^{210}Pb on ^{160}Dy at 1200 MeV. The dashed line is a traditional calculation with the dashed spectroscopic factor of Fig. 5, and the solid line is the squid effect calculation with the squid

spectroscopic factor of Fig. 5. Note the squid suppression of population around spin 10h.

Fig. 7. Classical quantum number functions at closest approach (solid line) and at the end of the collision (dashed line) for Pb on Dy at 1200 MeV. The spin at the diabolic (band-crossing) region is shown by the horizontal line labeled $I_{diabolic}$. The two roots for the diabolic spin at closest approach are indicated by vertical lines. Note that the forward root has a final spin nearly twice that at closest approach (as in the sudden approximation), whereas the back root has a final spin slightly lower than at closest approach, a dramatic consequence of the finite moment-of-inertia and rotation of the nucleus during the time of the Coulomb torque.

Fig. 8. Same as Fig. 6, except at the lower beam energy of 1100 MeV.

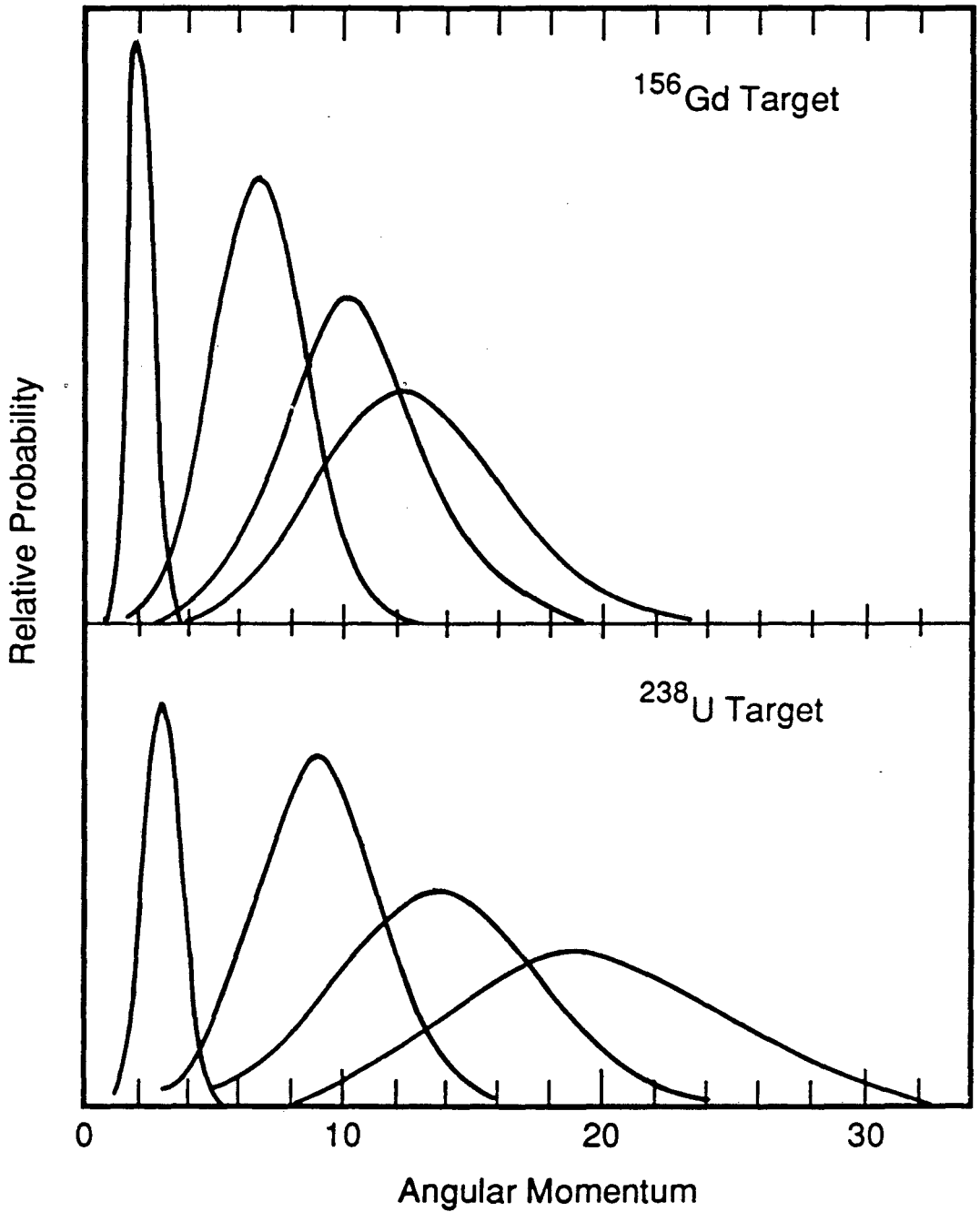
^{156}Gd Target
^{238}U Target
Relative Probability
0
10
20
30
Angular Momentum

Figure 1

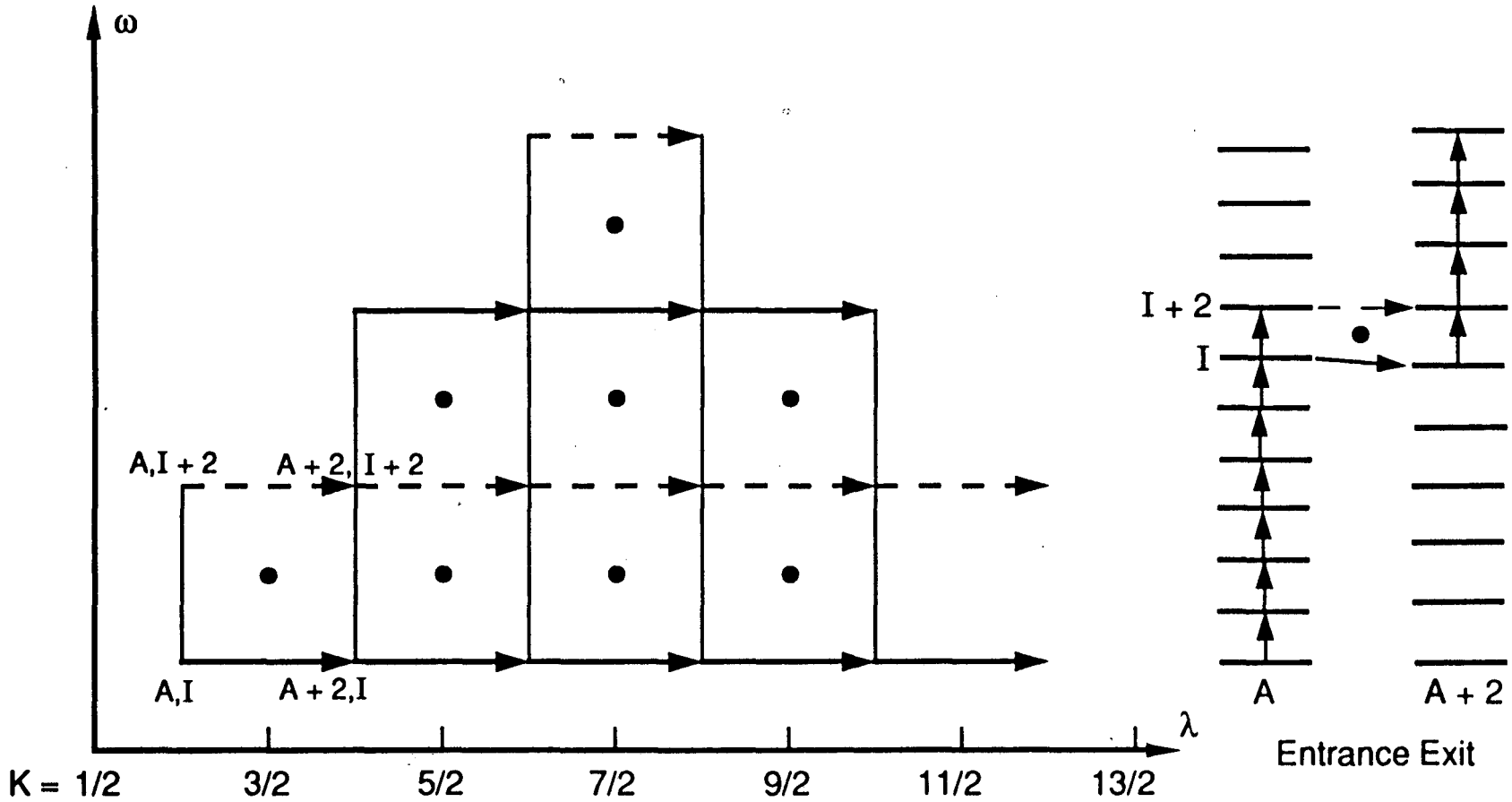

Figure 2

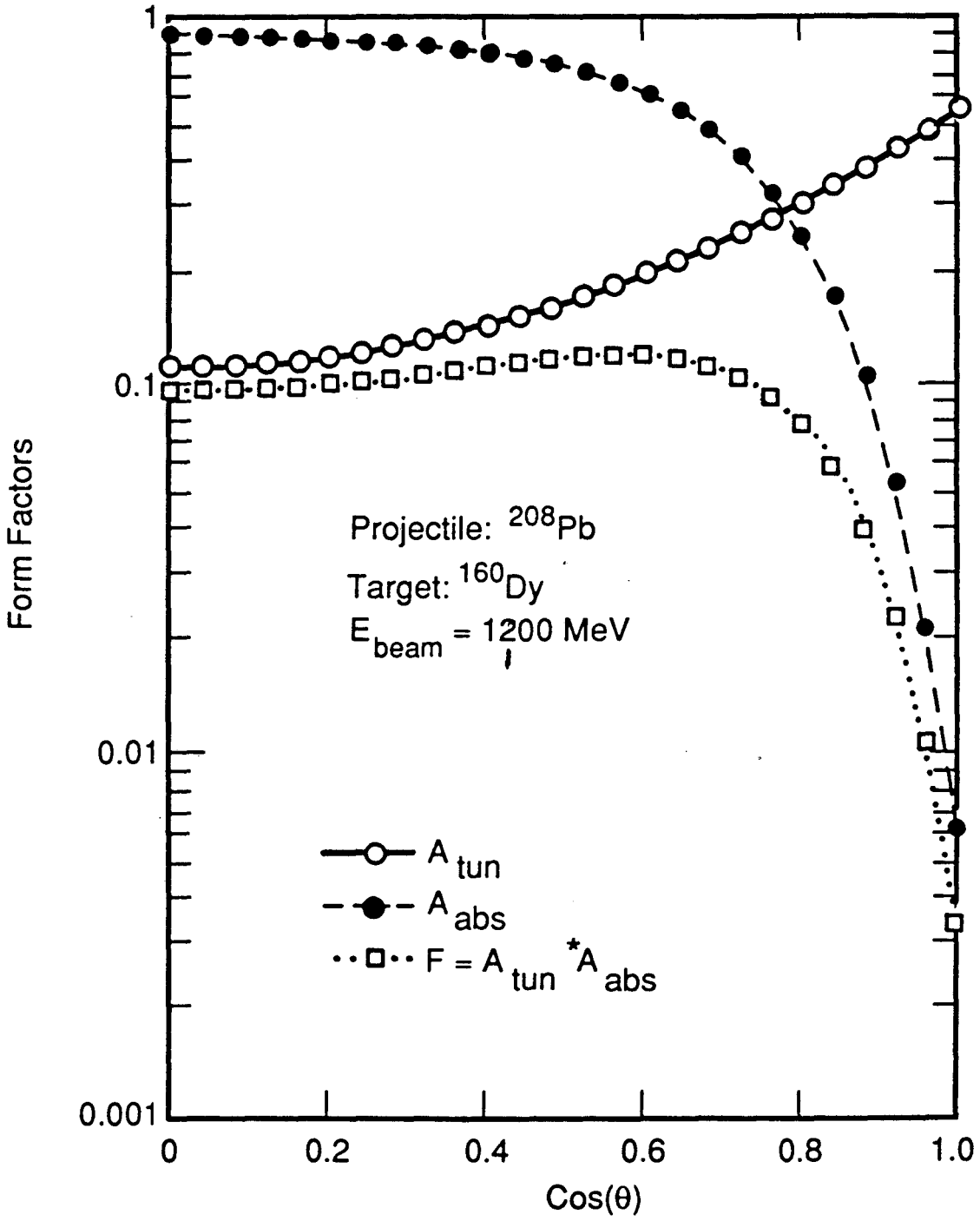

Figure 3

Rasmussen/Stoyer(9/15)-10

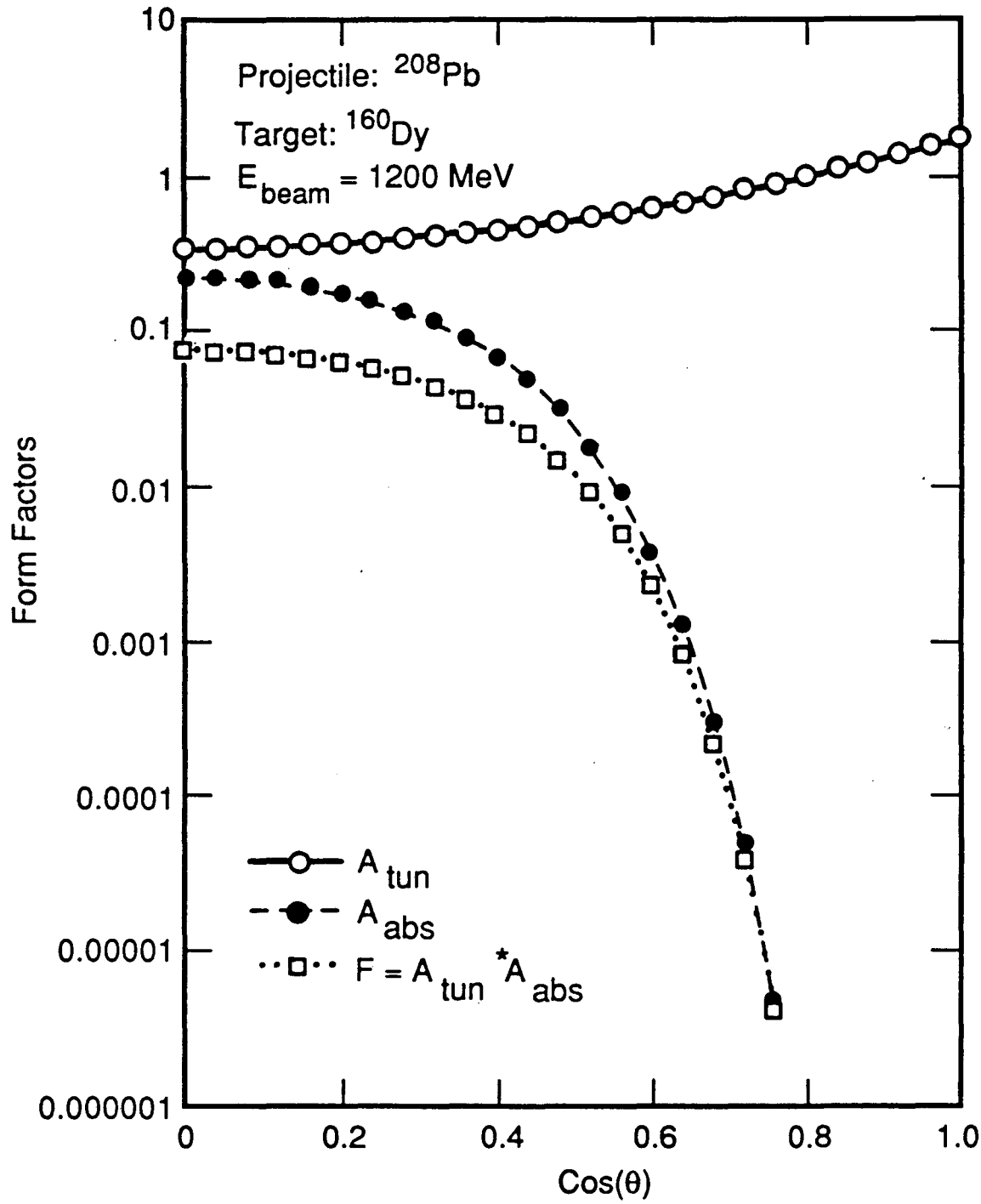

Figure 4

Rasmussen/Stoyer(9/15)-9

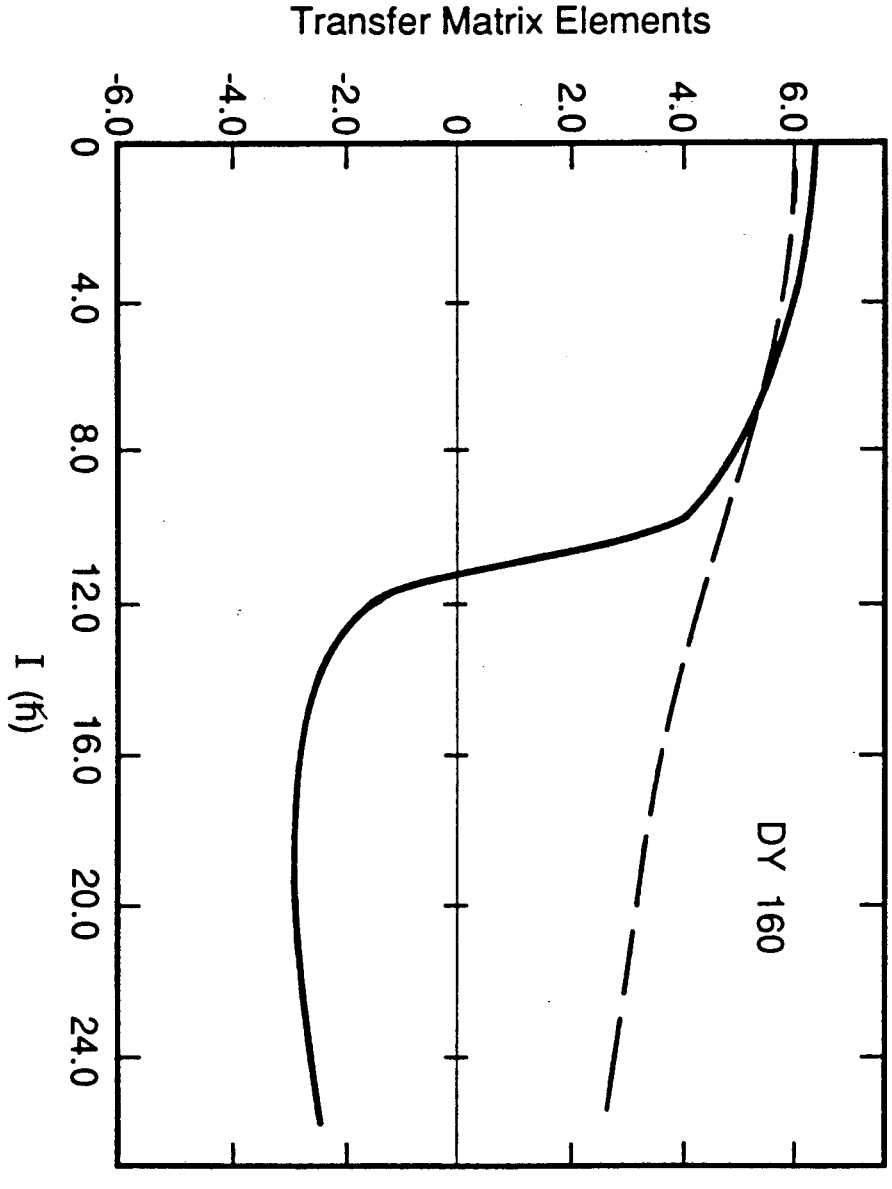
Transfer Matrix Elements
6.0
4.0
2.0
0
-2.0
-4.0
-6.0
DY 160
0
4.0
8.0
12.0
16.0
20.0
24.0
I (ħ)

Figure 5

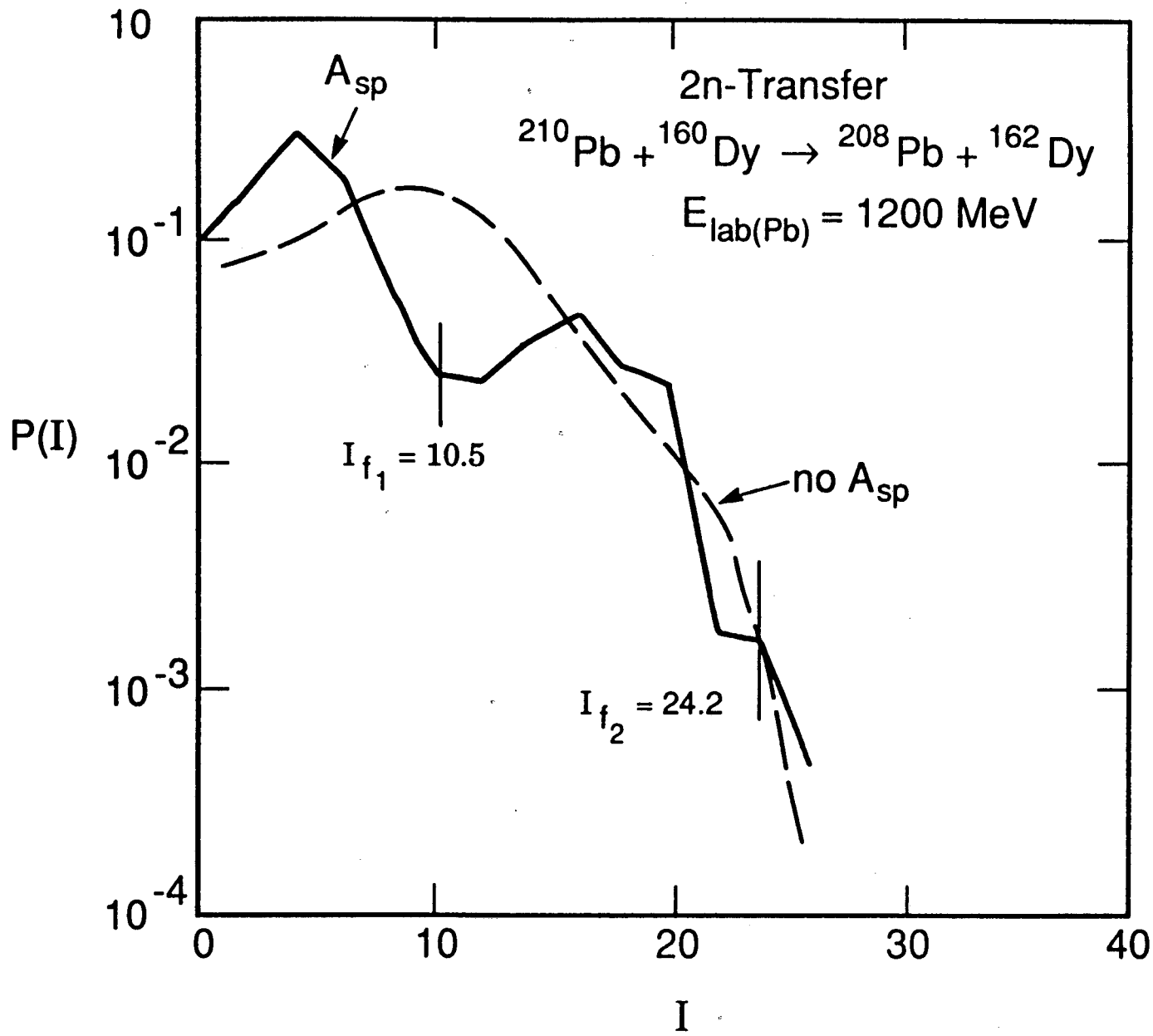

Figure 6

Rasmussen/Stoyer(9/15)-1

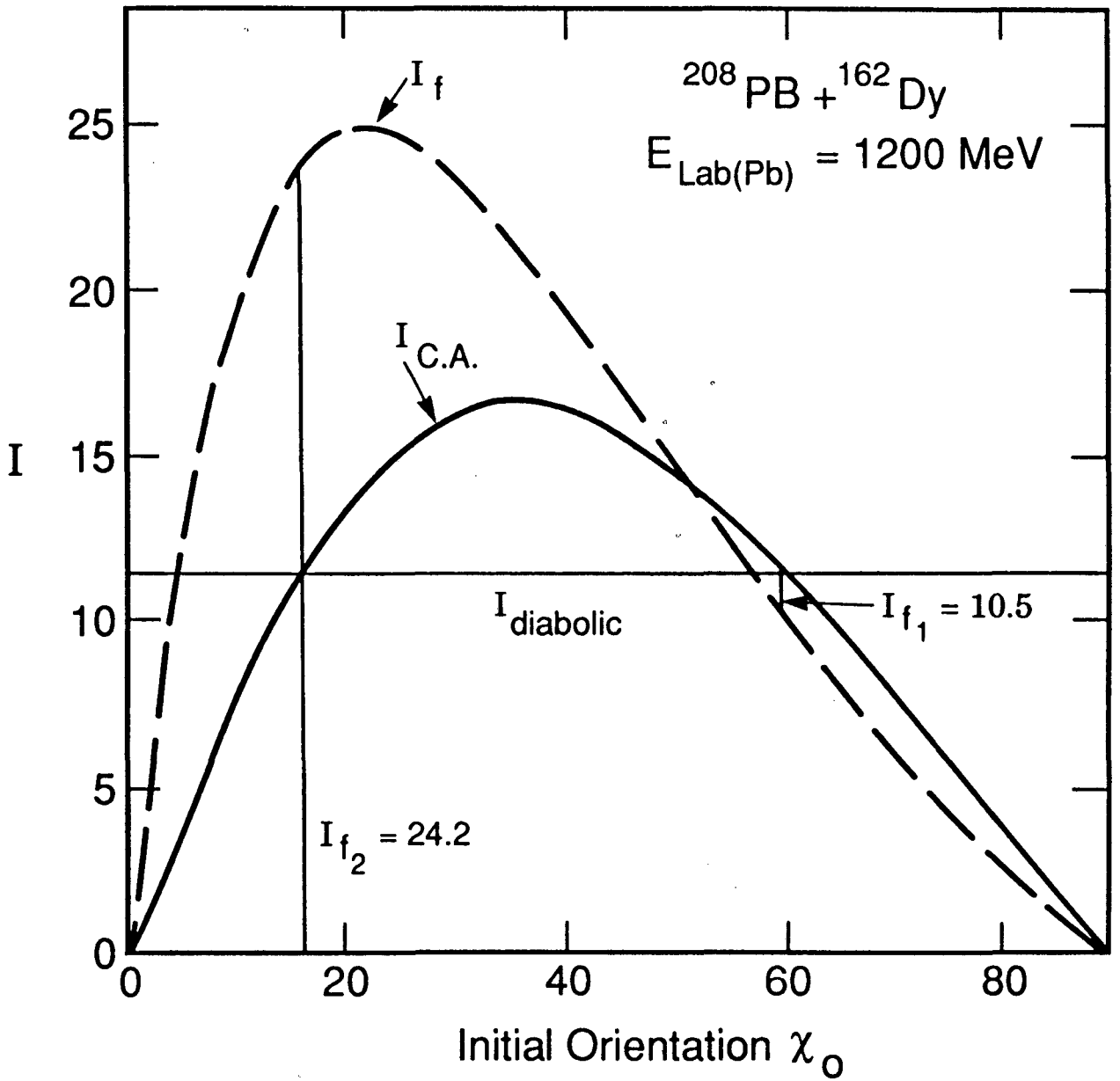

Figure 7

Rasmussen/Stoyer(9/15)-5

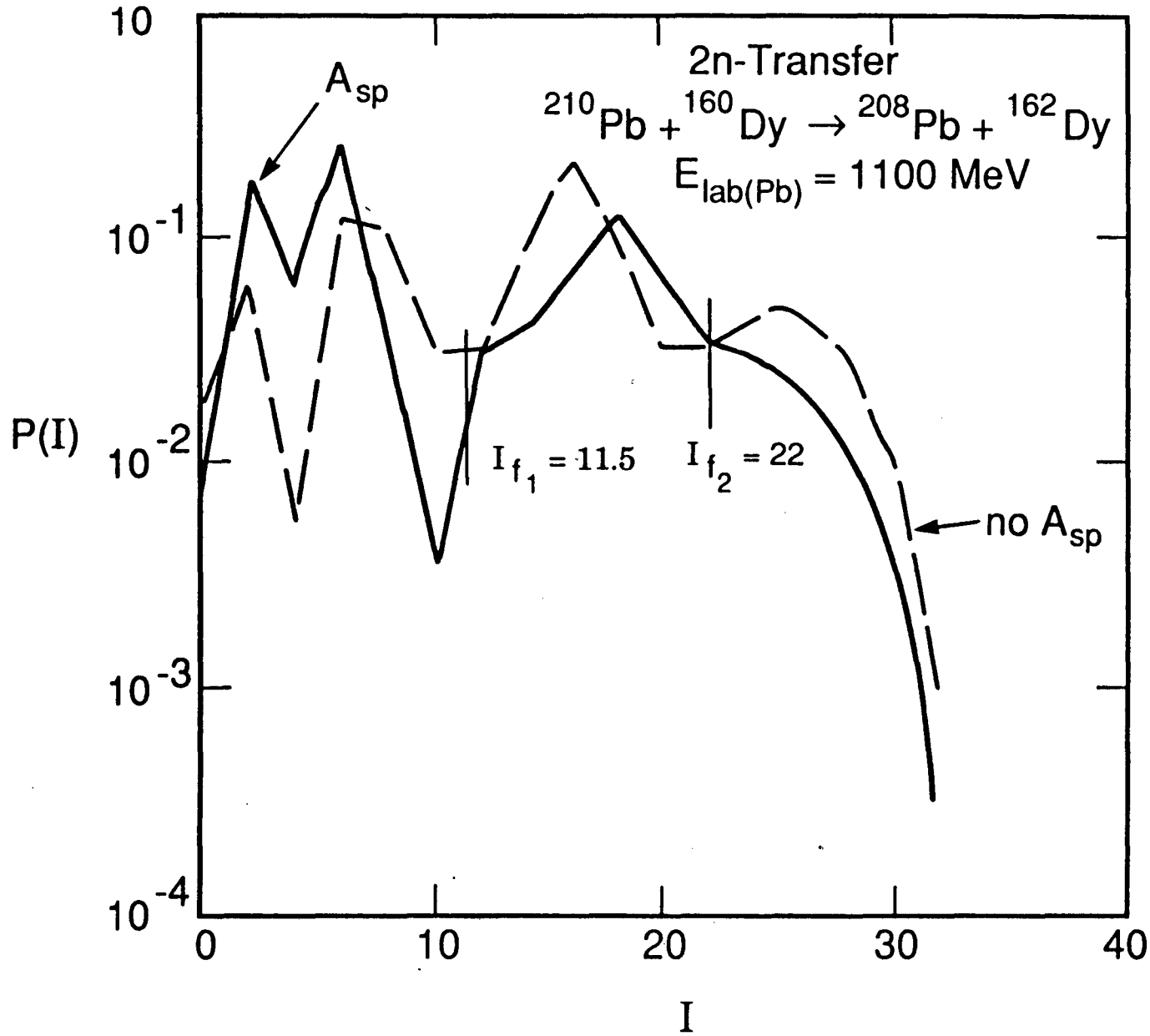

Figure 8

Rasmussen/Stoyer(9/15)-3

1. P.Ring and R.S.Nikam, Proc. Intern. Conf. on Microscopic theory of nuclear structure (Sorrento, Italy, May, 1986).

2. R.S.Nikam, P.Ring, and L.F.Canto, Z. Phys. **324** (1986) 241; Phys. Lett. B **185** (1987) 269. P.Ring, Proc. IX Workshop in Nuclear Physics, Buenos Aires (June, 1986) Macchiavelli, Sofia, and Ventura eds., World Sci. Press (1987) p. 143. P. Ring, Proc. Workshop on Microscopic Models in Nuclear Structure Physics, Oak Ridge, TN, Oct. 3-6, 1988, World Scientific Press, Singapore, p. 298.

3. L.F.Canto, R. Donangelo, R.S.Nikam, and P. Ring, Phys. Lett. B192 (1987) 4.

4. M.W.Guidry, T.L.Nichols, R.E.Neese, J.O.Rasmussen, L.F.Oliveira, and R.J.Donangelo, Nucl. Phys. **A361** (1981) 274.

5. P. Ring, "Berry's Phase and Diabolic Pair Transfer in Rotating Nuclei," in Proc. Workshop on Microscopic Models in Nuclear Structure Physics, Oak Ridge Oct.3-6, 1988, M.W.Guidry, J.H. Hamilton, D.H.Feng, N.R. Johnson, and J.B. McGrory, eds., World Scientific Press, Singapore, 1989.

6. M.V. Berry, Proc. Roy. Soc. **A392** (1984) 45.

7. C.Price, H.Esbenson, and S.Landowne, Phys. Lett. B 197 (1987) 15.

8. A.Winther and J. deBoer, "A Computer Program for Multiple Coulomb Excitation," Caltech Report, Nov. 18, 1965, in K. Alder and A. Winther, Coulomb Excitation, Acad. Press, NY (1966) p. 303.

9. J. de Boer, C.H. Dasso, and G. Pollarolo, Preprint, 1989.

10. M.W.Guidry, R.W.Kincaid, and R.Donangelo, Phys. Lett. 150B (1985) 265.

11. H.Emling, E.Grosse, R.Kulessa, D.Schwalm, and H.J.Wallersheim, Nucl. Phys. A419 (1984) 187.

12. P. Ring, Proceedings of the IV Jorge Andre Swieca Summer School in Nuclear Physics, Caxambu, Brazil, February, 1989.

13. G.Breit and M.E.Ebel, Phys. Rev. **103** (1956) 679 and Phys. Rev. **104** (1956) 1030.

14. M.W. Guidry, "Fermion Dynamical Symmetry and Nuclear Spectroscopy," this symposium (1989).

* Lawrence Berkeley Laboratory, Univ. of California,

Berkeley, CA 94720

** Inst. de Fisica - Universidade Federal do Rio de Janeiro,

C.P. 68528, Rio de Janeiro, RJ, BRASIL

% Department of Physics, Kuwait University, Kuwait
# Department of Physics, Univ. of Tennessee, Knoxville, TN 37996
and Oak Ridge National Laboratory, Oak Ridge, TN 37830
+ Physik Department, Tech. Univ. Munchen, Garching, Germany

LAWRENCE BERKELEY LABORATORY
TECHNICAL INFORMATION DEPARTMENT
1 CYCLOTRON ROAD
BERKELEY, CALIFORNIA 94720